Available online at www.CivileJournal.org

# Civil Engineering Journal

(E-ISSN: 2476-3055; ISSN: 2676-6957)

Vol. 10, No. 08, August, 2024

# Experimental Study on Seismic Performance of Kancingan Timber Frame Infill Walls Building

Sari Octavia [1*], Hartawan Madeali [1], Nasruddin [1], Mohammad Mochsen Sir [1]

[1] *Department of Architecture, Hasanuddin University, Gowa 92171, Indonesia.*

Received 03 May 2024; Revised 25 June 2024; Accepted 09 July 2024; Published 01 August 2024

**Abstract**

This study was carried out to examine the seismic performance of *Kancingan* house walls and the behavior of their timber frames, brick infill, and anchor nails during cyclic loading tests. *Kancingan* House, a timber frame building with brick infill walls, is a cost-effective and efficient method of wall construction commonly used in houses in Merauke, Indonesia. The experimental method was used to determine the seismic performance of the walls built using buswood with a module width of 100 cm and a height of 130 cm through cyclic load testing. The result showed a maximum lateral load of 26.43 kN with a displacement of 19.08 mm under compression loading and 28.78 kN under tensile loading with 15.6 mm displacement. The initial stiffness was measured at 5.03 kN and 9.59 kN/mm for compressive and tensile loading, respectively. Furthermore, ultimate load and displacement of 21.14 kN and 23.02 kN were obtained at a displacement of 30.68 mm under compressive loading and 25.23 mm under tensile loading. The ductility values of 10.76 and 9.78 were obtained under compressive and tensile loading. In conclusion, the study found that each wall element supports the seismic performance of the structure. As opposed to the timber frame, the infill walls have not suffered much damage except a hair crack because of the presence of anchor nails that keep the infill wall from collapsing when it loses its bond with the timber frames.

*Keywords:* Kancingan House; Timber Frame; Infill Wall; Merauke.

## 1. Introduction

The construction of timber frame infill walls is in high demand in some developing countries due to the economic advantages and seismic resilience, which are considered better than local unreinforced brick buildings. These structures offer a wide range of infill materials, which serve areas with varying degrees of seismic sensitivity [1–4]. In countries such as Europe, Asia, and Australia, different types of timber frame infill walls with distinctive characteristics and construction materials are commonly found [3, 5]. Typical examples include stone and brick infills [3], sagoo fronds, also called *Gaba-gaba* [6], etc. Meanwhile, certain types of timber-framed buildings with infill walls have unique features and names in different areas. For instance, in China, it is known as the *Chuan-dou* house [7, 8], with a timber frame made of wooden log and stone infill walls plastered with mud. In Turkey, the building is called *Himis* [9, 10], while in Portugal, it is referred to as *Pombalino*, where diagonal wooden members are used as bracing [11].

The use of timber frame infill walls, also called the Kancingan house in Indonesia, was found in Merauke, one of the cities in Papua Province, as shown in Figure 1-a. Octavia et al. [6] and Topan et al. [12] stated that due to the cost-effectiveness and efficiency, timber frame infill is widely used to construct walls in Merauke community houses. The building method combines two orthotropic and isotropic materials with contrasting physical properties, namely wood and brick [6, 12-14]. The process includes the installation of a timber frame and brick infill walls, resembling *dikancing*

* Corresponding author: sari@unmus.ac.id

http://dx.doi.org/10.28991/CEJ-2024-010-08-06

or buttoning. Based on field observations, the construction methods are not limited to residential buildings; rather, they comprised churches, schools, hospitals, offices, warehouses, and other public facilities.

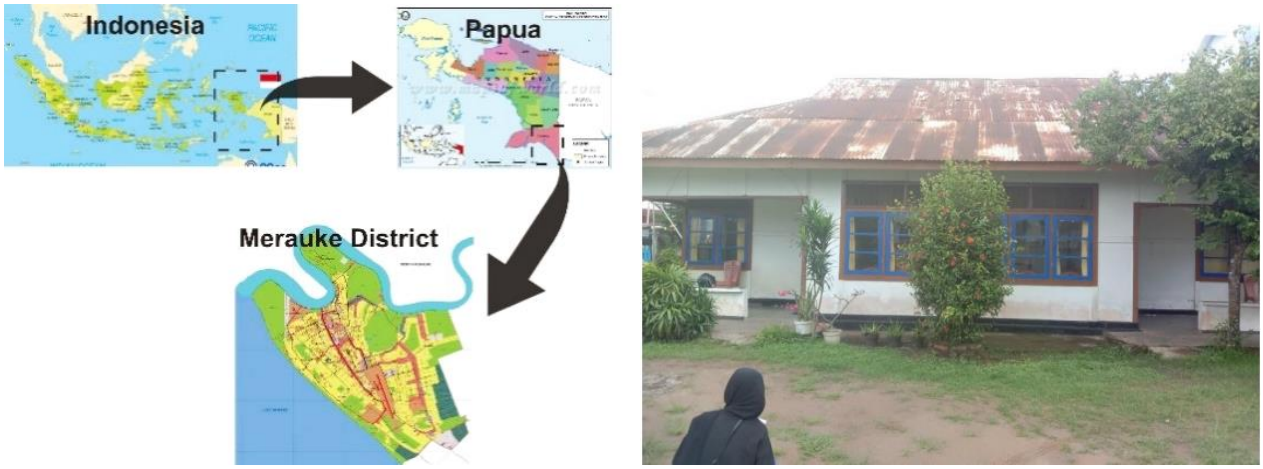


**Figure 1. (a) The Location of *Kancingan* house (b) *Kancingan* House built in 1960s**

The construction of a *Kancingan* house with a timber frame and brick infill walls tends to be durable. This is exemplified by the houses of the Dutch government shown in Figure 1-b. Despite being built in 1960, it had remained solid and completely functional under the management of the local government.

The *Kancingan* house has profound historical significance in the Merauke community, a heritage diligently preserved through the ages. According to Topan et al. [14], development led to changes in the construction process, modifying the functions of the building aspect that was once considered to be a strong structure. This was influenced by cost, materials, culture, and construction intricacy. In addition, the current model of the *Kancingan* house is shown in Figure 2.

**Figure 2. *Kancingan* house in Merauke**

Three types of building materials, namely wood, bricks, and nails were used to construct the walls. These materials, each with distinct physical properties, play critical roles in the structural integrity of the building. However, wood contrasts with the isotropic nature of the bricks because it is an orthotropic material. Nails were used as connertors on joints and anchors in the interface between brick and timber frames. The walls of the *Kancingan* house, a prevalent building in Merauke, are characterized by diverse materials and timber frame models.

### 1.1. Type of Material Used

There are three types of material used in *Kancingan* houses:

- ***Wood***

Wood is a natural resource that is a sustainable replacement for fossil fuels [15, 16] and a key component of green architecture due to the numerous benefits. A unique property is the orthotropic nature, which differs significantly from isotropic materials such as concrete and steel comprising three axes, including longitudinal, tangential, and radial [17]. Additionally, three main types of wood, namely *besi*, *rahay*, and *bus*, are commonly used as building materials. The selection process is largely influenced by the availability of besi wood by the government, thereby restricting the usage in *Kancingan* houses.

- ***Masonry Brick***

Masonry brick walls are characterized by relatively poor seismic performance despite their widespread use in developing countries, particularly in rural and suburban areas. This was mainly due to the low construction costs, availability of local materials, and lack of highly skilled labor [18], thereby leading to the reinforcement with concrete, steel, or wood. The locally produced bricks used in *Kancingan* house had dimensions of 10 × 20 × 5 cm, printed and manually fired without the use of a hanger. These were mounted at 1/4 stone width, resulting in masonry walls relatively thin compared to houses constructed with concrete.

- ***Nails***

Nails are typically metallic materials that serve as reinforcing stiffeners for wooden joints, a subject that has received considerable attention in numerous studies [19, 20]. However, because wood and brick possess distinct physical properties, nails are used as anchors to bind the timber frame and infill wall.

### 1.2. Timber Frame Pattern in *Kancingan* House

The architectural design of the *Kancingan* House features wooden columns and a wall frame, known as a regel, measuring 8/8 cm in size. The design of the door and window frames significantly impacts the appearance of the walls (Figure 3-a). Additionally, these walls possessed a variety of grid patterns and module sizes characterized by the vertical spacing of the timber frames. The horizontal beams were placed in line with the heights of the door and window frames, while the vertical ones coincided with the wall length (Figure 3-b).


**Figure 3. (a) A pattern of windows and doors frame that often appears in *Kancingan* house, (b) Timber frame pattern on wall in *Kancingan* house**

Several studies have been conducted on timber-frame buildings with infill walls; for example, Psycharis et al. [21] examined the seismic behavior of the Berykiou house in Lefkas, while [7, 8, 22, 23], investigated the traditional Chuan Dou in China. Similarly, Previous studies [9, 10, 24] analyzed the structural features of Himis in Turkey. The study conducted by Hejazi et al. [25], focused on examining the seismic performance of timber frame walls with fired brick infill, and Shen et al. [26] investigated the seismic resistance of traditional Chinese houses constructed using timber frames with stone infills and mud. Furthermore, Makarios & Demosthenous [27] studied the seismic responses of a traditional house in Lefkas, Greece, while Poletti & Vasconcelos [28] explored the seismic behavior of timber frames with various infills, including masonry brick, lath, and plaster walls, as well as timber frames without infills. The study by Ruggieri & Zinno [29] focused on the construction system of Borbone in Italy, while Xu et al. [30] examined the traditional timber-frame infill wattle and daub.

Recently, experts have suggested using various building materials, such as partitioned infill walls [31], similar to the model found in the *Kancingan* house in Merauke. Cheng et al. [3] and Ren at al. [7] stated that partitioned infill walls generally have a high ductility capacity, low damage characteristics even at large deviation values, and show weak interaction between the frame and the brick pair material. However, Cheng et al. [3] and Ren at al. [7] identified unresolved gaps, particularly concerning the openings needed for doors and windows for lighting and ventilation purposes, which are closely related to the patterns of horizontal and vertical timber frames on the walls, as well as the seismic performance of structures, a challenge also observed in the *Kancingan* house. Recent studies have focused on the importance of addressing this problem or gap, especially for houses in tropical areas such as Indonesia, thereby making the *Kancingan* House an interesting topic for further investigation.

Specifically on the study of the *Kancingan* house, Topan et al. [12] explored the architectural aesthetics of the *Kancingan* house, while Octavia et al. [13] analyzed the feseability of the structures. Octavia et al. [32] compared the semi-permanent houses, which use steel as construction material. However, no preliminary study had examined the seismic performance of the *Kancingan* house, irrespective of the high earthquake risk the region poses in Indonesia.

Based on previous investigations, the current study aimed to address the identified gaps by determining the seismic performance of the walls in the *Kancingan* house. In addition, it seeks to analyze the behavior of the timber frame, brick infill wall, and nails as connectors on joints and nails as anchor through a series of experimental tests. These efforts reflect the state-of-the-art study and the originality of focusing on regions vulnerable to seismic earthquakes and dew, such as Merauke.

Various methods were used to test the seismic performance of buildings, including numerical [33-35] and experimental methods [23, 29, 30, 36]. This present study adopted experimental methods, specifically cyclic load tests, to simulate earthquake conditions. This included increasing the load or deformation pattern based on predetermined or subsequently derived load distribution from the response of the measured specimen. The following parameters peak, and ultimate loads, ductility, stiffness, and dissipation energy, were assessed during the testing process.

## 2. Material and Methods

Figure 4 shows the flowchart of the study, starting with problem identification, followed by a literature review and experimental stages to obtain the results. An experimental method was adopted, including the use of cyclic loading to assess the seismic performance of walls in the *Kancingan* house.

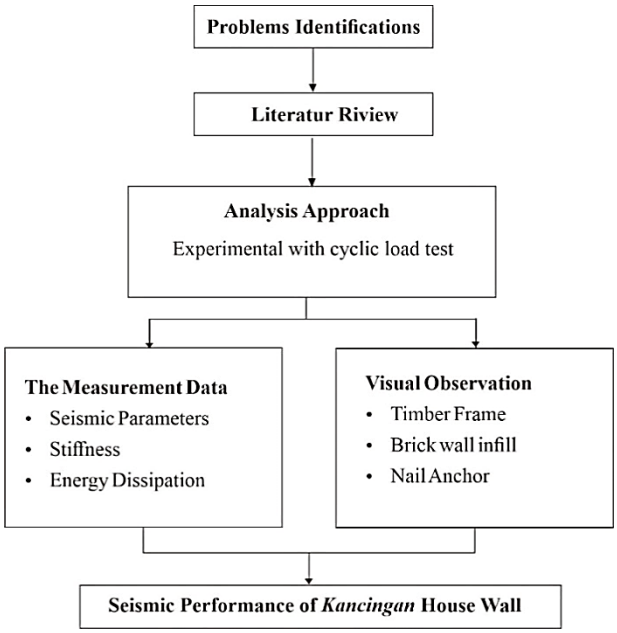


**Figure 4. Flowchart of the research**

The present study was conducted using an experimental method, following a quantitative design. According to Kuantitatif [37], an experimental method entails using an experiment to determine the effects of independent variables or treatments on dependent variables or outcomes under controlled conditions. In this study, wood, bricks, and nails were selected as independent variables, while seismic performance obtained through testing with cyclic loads served as the dependent variable.

A field survey was conducted on *Kancingan* house in Merauke District, Papua Province, Indonesia. The aim was to obtain information on the commonly used wood materials, height and width of the wall frames, wood dimensions, and type of connection used in most houses. Based on the surveyed samples, wood, masonry brick, and nails were selected for further analysis. Furthermore, the seismic performances were tested at the structure and material laboratory of Hasanuddin University, Makassar, Indonesia. This was aimed to determine a model of the test specimen representing the on-site *Kancingan* house, and the procedure is stated as follows:

### 2.1. Specimen

The specimen designed for this experiment is similar to the wall construction process in a *Kancingan* house. It comprised a timber frame made of bus wood *(malelauca cajuputi),* with dimensions of 2x100 cm module width and 130 cm height. As shown in Figure 5, wood sizes 8/8 and 4/8 were used for the main column and divider beam, respectively. The type of connection implemented was the mortise and tenon joint, positioned at the top of the specimen and commonly found in traditional households, namely the Balinese house [38], as shown in Figure 6-a. Additionally, a halved-joint connection was used at the base of the sample connection, as shown in Figure 6-b.

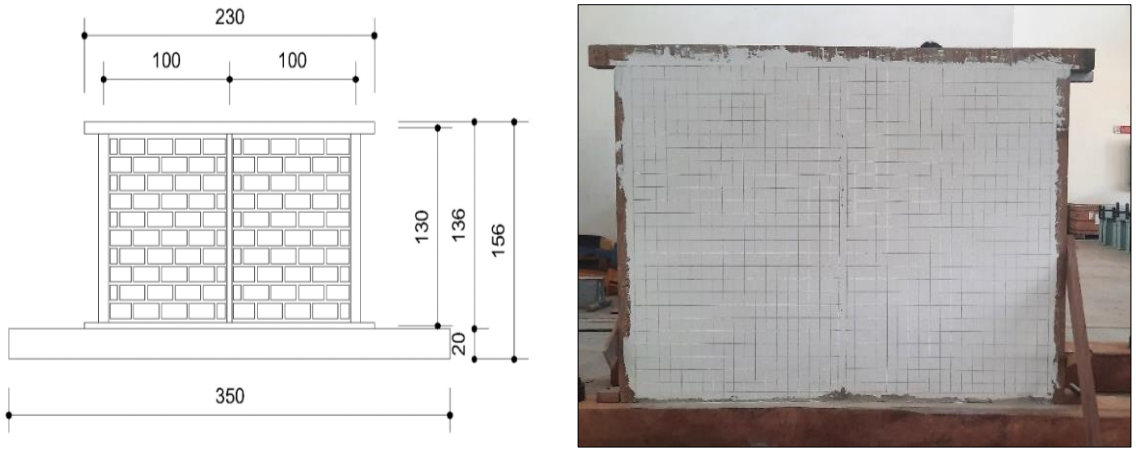


**Figure 5. The specimen of *Kancingan's* wall**

**Figure 6. (a) Mortise and tenont joint. (b) Halved joint**

A frame was made before the installation of the walls, and a spooning 1 cm deep was carved on the timber. Furthermore, a 10 cm nail was mounted, as shown in Figure 7-a, at a distance of 30 cm and 10 cm on the vertical and horizontal wooden beams, respectively. The nail was an anchor, connecting the timber frame to the brick. The joint on the timber frame was reinforced with nails, and the brick wall was gradually built. Specifically, after every three layers, the installation was stopped for a moment to allow the newly mounted brick pair and the cement mixture to dry. The process is continued until the entire brick wall is installed on the wooden frame.

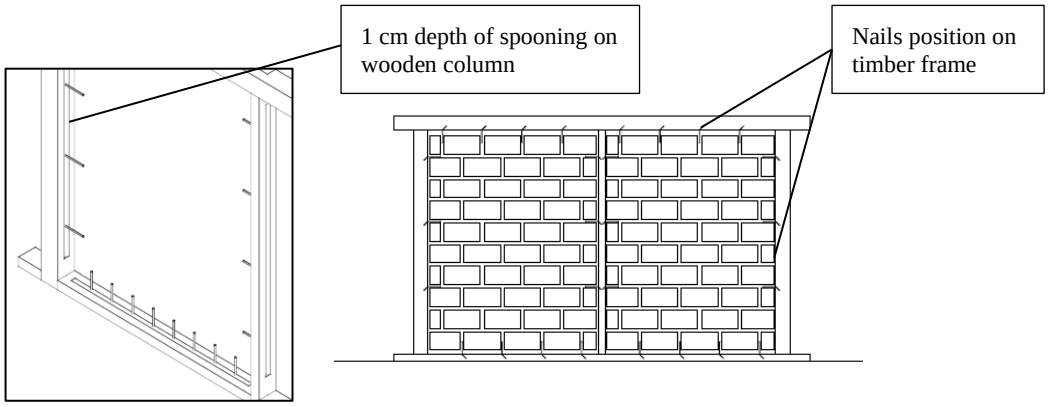


**Figure 7. (a) The spooning on timber frame. (b) The nail position on the timber frame**

Following the installation of the brick walls on the specimen, as shown in Figure 8, a curing process was initiated for one week to ensure proper hydration of the cement before plastering. The plastering process was performed with a mortar composed of one part cement and four parts sand on both sides of the wall, resulting in plaster and final thicknesses of brick infill approximately 1.5 cm and 8 cm, respectively. Subsequently, the walls were covered with wall filler or putty to facilitate the placement of 5 × 5 cm grid lines, which aided in detecting cracking during the test. The specimens were cured for 28 days to ensure the cement was well-hydrated and deemed ready for the lateral-load test.

**Figure 8. Process of installing a brick wall**

## 2.2. Test Method

The ASTM E 2126 test method B "ISO 16670 (ISO 2003)" [39], a widely recognized standard, was used to evaluate the shear resistance of building walls under cyclic (reversed) loading conditions. In addition, the specific test scheme is shown in Figure 9.

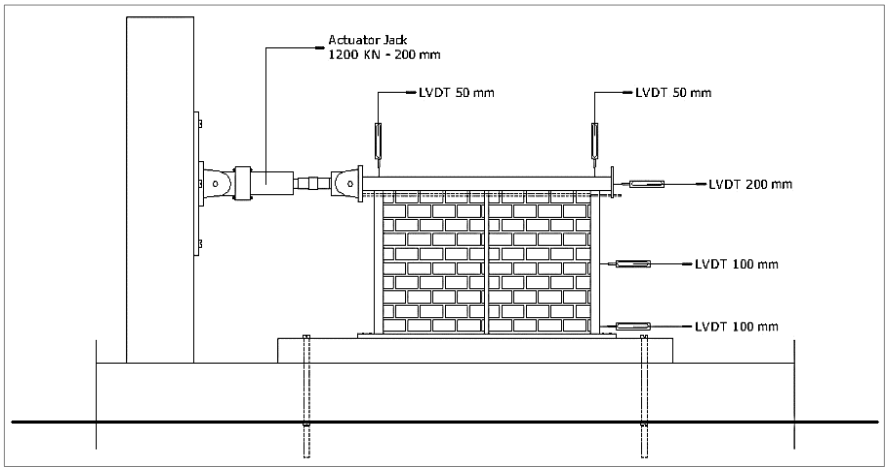


**Figure 9. Test Scheme according to ASTM E 2126**

The cyclic displacement of the actuator jack must be regulated in a specific procedure according to ASTM E 2126 test method B [39]. During the loading process, a transformation cycle is continuously escalated in the displacement phase to reach the designated level. The ISO loading schedule comprised two displacement patterns, as shown in Figure 10. The first pattern consisted of five completely inverted single cycles at displacements of 1.25%, 2.5%, 5%, 7.5%, and 10% of the $\Delta_m$ final value. The second pattern comprised phases, each containing three reverse cycles of equal amplitude at displacements of 20%, 40%, 60%, 80%, 100%, and 120% of the ultimate displacement $\Delta_m$.

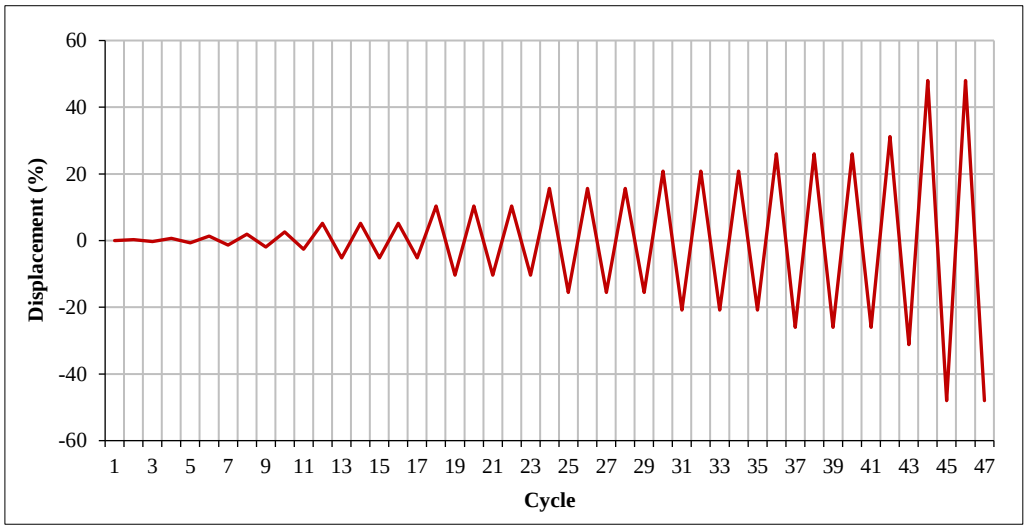


**Figure 10. Loading cycle**

### 2.3. Device Set Up and Specimen

The specimens ready to be tested were placed on the device according to the arrangement shown in Figure 11.

**Figure 11. Set up tools and test objects**

The LVDT and strain gauge were installed on the specimen at a specified location and connected to a data logger and computer to measure the load and displacement during the test. Data were collected intermittently from the logger and computer throughout the test duration. Visual observations, such as identifying the first crack, the patterns, and breadth, were documented directly on the specimen during the test. Finally, the behavior of the walls was assessed based on these observations and measurements.

## 3. Result and Discussion

Computer data and instrumentation were further used to generate hysteretic and envelope curves, aiding the determination of the seismic parameters of the specimen during testing.

### 3.1. Hysteretic Curve

The graph in Figure 12 shows the relationship between the lateral cyclic loads and the displacement of the specimen. The hysteretic curve of the specimen resembles the shape of the number 8, with the ends being larger than the waist, showing a pinching effect due to decreased stiffness on the structure caused by lateral loads. As the displacement increased beyond 10 mm, the shape of the curve became more regular, displaying a Z-like appearance. This suggested that the horizontal movement of the test object was a result of the incompatibility between the infill wall and timber frame, arising from the use of two different materials in the walls [40].

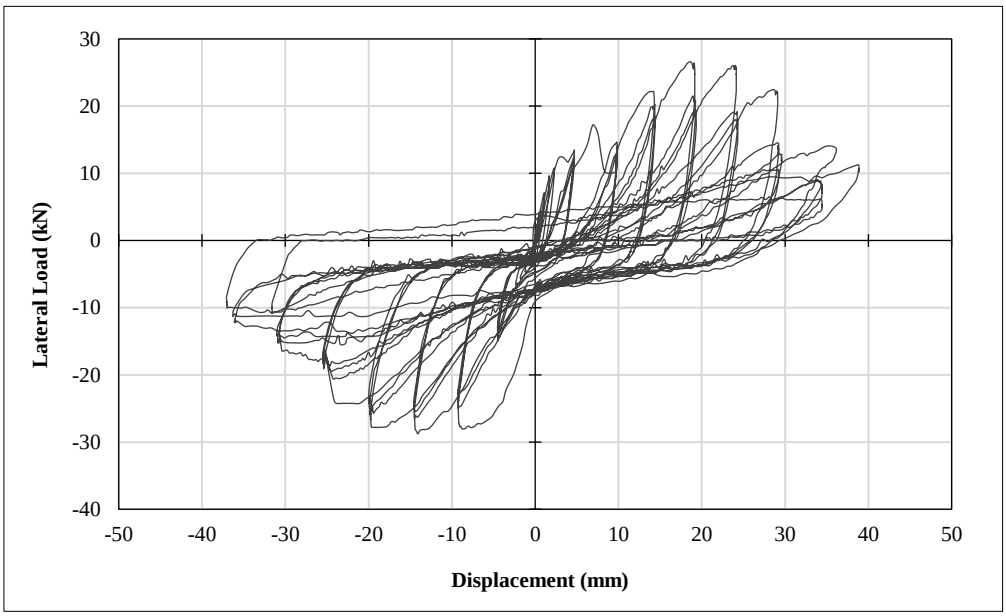


**Figure 12. Hysteretic curve**

Based on the hysteretic curve, the test specimen reached the maximum load of 26.43 kN at a drift of 73,3% cycle, with a displacement of 19.08 mm in the compressive loading. For the tensile loading, the specimen experienced the highest load of -28.78 kN at a drift of 60% cycle, with a displacement of -15.60 mm. The substantial displacement capacity showed that the structure can withstand earthquakes by displacing capacity rather than structural strength, as observed in the building research at Lefkas [21]. Meanwhile, the maximum load value and ductility ratio >20 kN and >10, respectively, it implied that the structure is resistant to earthquake loads [26].

## 3.2. Envelope Curve

The envelope curve in Figure 13 shows the maximum load experienced in each cycle. This representation is accompanied by a bilinear curve based on the equivalent energy elastic–plastic (EEEP) method, as described in ASTM E 2126. The variables along the curve, such as the elastic stiffness ($K_e$), Yield Load ($P_y$), Peak Load ($P_{peak}$), ultimate load ($P_u$), and ductility of the specimen, provide invaluable information regarding the performance of the material during cyclic testing, as shown in Figure 13.

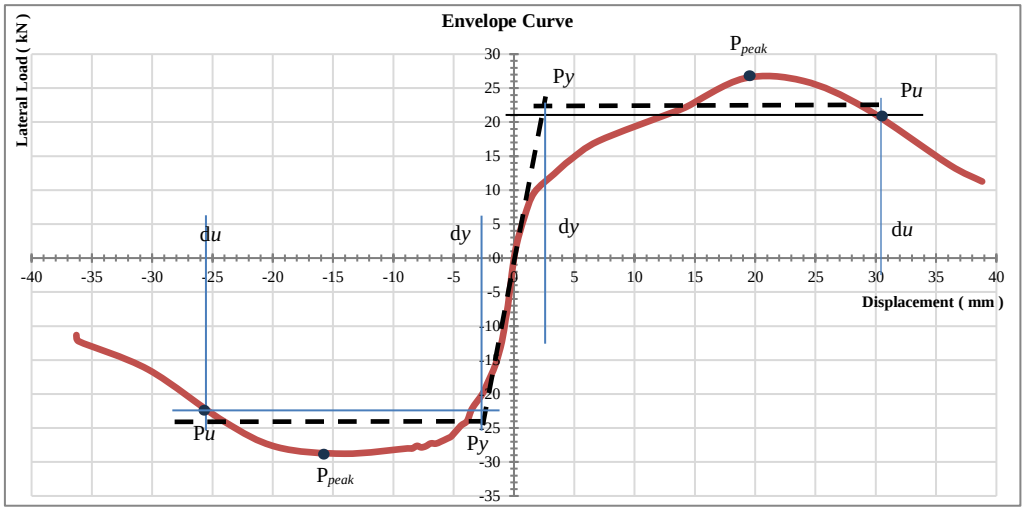


**Figure 13. Envelope curve**

Next, the seismic parameters shown in envelope curve:

The elastic stiffness was calculated as the slope of either the free displacement or envelope curve at a load of 0.4 peak. In addition, this slope was used to define the elastic part of the curve. The elastic stiffness was calculated using the following formula:

$$Ke = \frac{0.4\ Ppeak}{\Delta\ 0.4\ Ppeak} \quad (1)$$

where $K_e$ elastic stiffness (KN/mm), $P_{peak}$ Peak load, $\Delta$ 0.4 $P_{peak}$ displacement on 0.4 $P_{peak}$.

When examining the elastic stiffness of the specimen subjected to compressive and tensile loads of 5.03 and 9.59 kN, respectively, it was observed that the higher the value of elastic stiffness, the greater the capacity of the wall to sustain the lateral force (P) when operating under elastic deformation.

- ASTM Standard 2126-11 was used to determine the load under the yield condition using the elastic-plastic equivalent energy (EEEP) method. The findings showed that in the compressive loading direction, the yield load ($P_y$) and displacement ($D_y$) of the test object was 22.47 kN and 2.85 mm, respectively. Additionally, in the tensile loading direction, $P_y$ and $D_y$ were 22.46 kN, and 2.58 mm.
- The ultimate load, $P_u$, is generally defined as the load achieved at 80% of the peak load. In the compressive loading direction, the ultimate load is 21.14 kN at displacements of 30.68 mm. However, in the tensile loading direction, the ultimate load is 23.02 kN and displacements of 25.23 mm.
- The capacity of a structure to withstand deformation or permanent changes in shape when subjected to repeated or cyclic loads is referred to as ductility. In this study, the ductility of the test specimens was assessed in both compressive and tensile loading directions. The ductility in the compressive and tensile directions are 10.76 mm and 9.78 mm, respectively. The average ductility ratio of the test object is 10.27, which indicates the resistance of the structure to seismic load. This is particularly important in the seismic area because it provides an estimate of the structure's capacity to deform nonlinearly even after approaching ultimate resistance without significant loss of strength.

Table 1 shows the overall seismic parameters.

**Table 1. The seismic parameters**

| Loading direction | $K_e$ (kN/mm) | $P_y$ (kN) | $D_y$ (mm) | $P_{peak}$ (kN) | $D_{peak}$ (mm) | $P_u$ (kN) | $D_u$ (mm) | Ductility μ |
|---|---|---|---|---|---|---|---|---|
| Compressive | 5.03 | 22.47 | 2.85 | 26.43 | 19.08 | 21.14 | 30.68 | 10.76 |
| Tensile | 9.59 | 22.46 | 2.58 | 28.78 | 15.6 | 23.02 | 25.23 | 9.78 |
| Average | 7.31 | 23.46 | 2.72 | 27.61 | 17.34 | 22.08 | 27.96 | 10.27 |

### 3.3. Failure Pattern on Specimen

Figure 14 shows the failure patterns of the test specimen, and during the initial phase of the testing, the curve displayed stability with no signs of pinching. However, in the sixth cycle, at a 20% drift, a narrowing on the waist or pinching effect was observed, indicating that the test specimen became weak at the joints, due to the detachment of masonry infill from the frame [41]. This was further observed in the seventh cycle, where a 40% drift resulted in the wooden column being lifted 5 mm from the connection, leaving a 3 mm gap between the upper brick wall of the specimen and the horizontal wooden beam, as shown in Figures 14-a and 14-b.

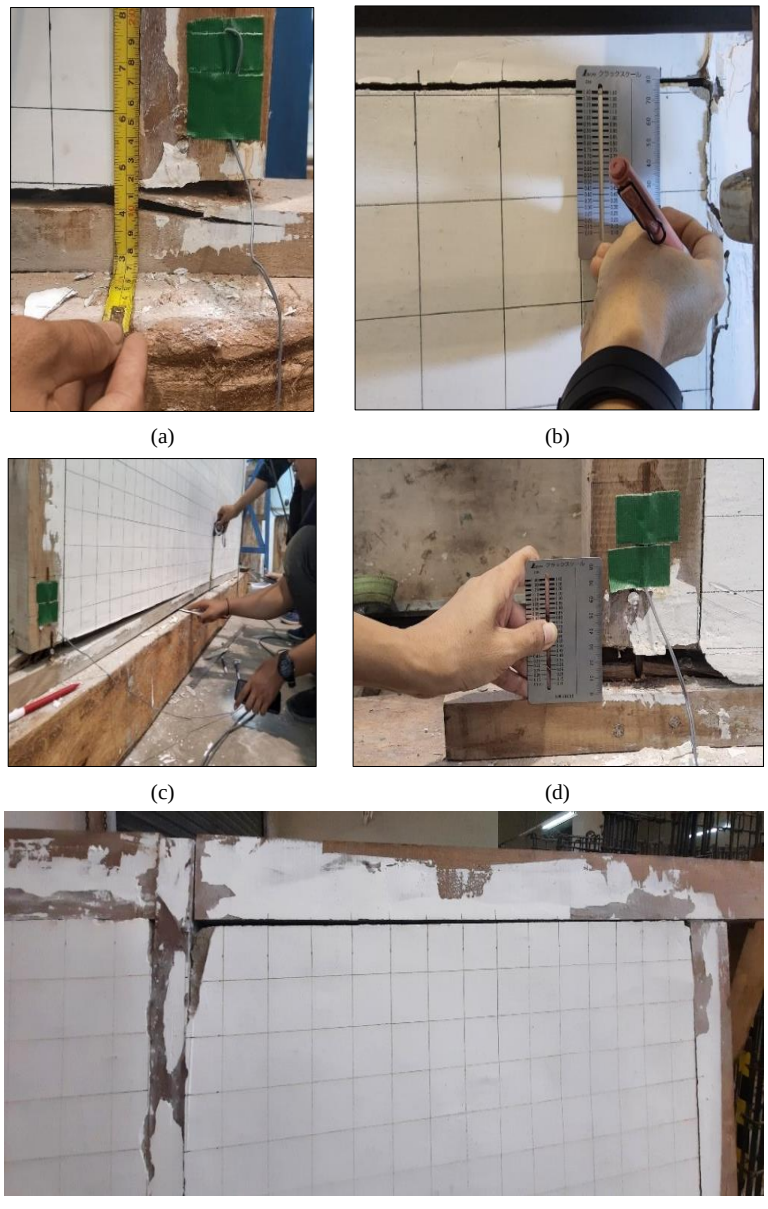

**Figure 14. Failure pattern on specimen, (a) failure on wooden column joint, (b) the gap between timber frame and infill brick wall, (c) the infill wall brick behaviour during the test, (d) the last cycle of the test, (e) the condition of specimen after the cyclic test**.

Nail pull-through or shearing failure becomes noticeable on the wooden connection at a 54% drift and 14.22 mm displacement, visible on the 5 mm lifted brick wall and the 18 mm raised column, as shown in Figure 14-c. This deformation occurs due to structural damage, mainly caused by nail failure as the connecting tool in the wood joints. The nail as the connecting instrument contributes to the lateral resistance system of the timber frame structure [42], and to improve the performance of the joints, either by incorporating steel plates [43] or replacing nails with self-tapping screws [44].

The increase in the loading cycle decreases the distance between the wooden columns, including the gap between the connections of the brick walls and the timber frame, which also increases, as shown in Figure 14-e. The gap formation results from the lack of bond between these two types of materials, leading to the separation of the infill brick wall from the interface of the frame [45]. This phenomenon becomes visible when the movement surpasses 10 mm, marked by the appearance of a pinching effect on the hysteretic curve, indicating the loop forming a narrowing of the waist.

The most significant damage occurred at wood connections fortified with nails, leading to the deformation of the walls aligns with Vasconcelos et al. [46] and Vieux-Champagne et al. [47]. In the eleventh cycle drift, reaching 118 %, the wooden column lifted from the joint approximately 30 mm and 28 mm in the compressive and tensile loading directions, respectively, as shown in Figure 14-d. Figure 14-d showed that this condition resulted in rocking motion of the wooden column, thereby leading to structural failure and the termination of the test. The failure model of the structure varies depending on the infill materials, such as stone and clay mud. Shen et al. [26] the inconsistency between the timber frame and the infill wall using stone and clay mud was discovered to be the main reason for the wall collapse, without damage to the timber frame. However, the timber frame failed in this study while the infill wall remained intact.

The pattern of cracks on the specimen and the behavior of the wall during the test resembled the ones in Figure 15-a. Cracks started to appear in the wall at the fourth cycle drift, registering at 6.46% with a load of 9.63 kN and a displacement of 1.68 mm. The crack continued to appear until the 11th cycle drift reached 104%. While cracks were evident during the test, it was mostly hairline, with shear failure occurring at the interface between the timber frame and the infill wall. When the infill walls are detached from the wood, it only serves as filling and stiffeners rather than load distributors, preventing the cracks from not causing the wall to collapse. In addition, Langenbach [48] stated that the division of the walls into smaller panels equipped with columns, horizontal beams, and mortars of poor quality helped prevent the development of large cracks in the wall.

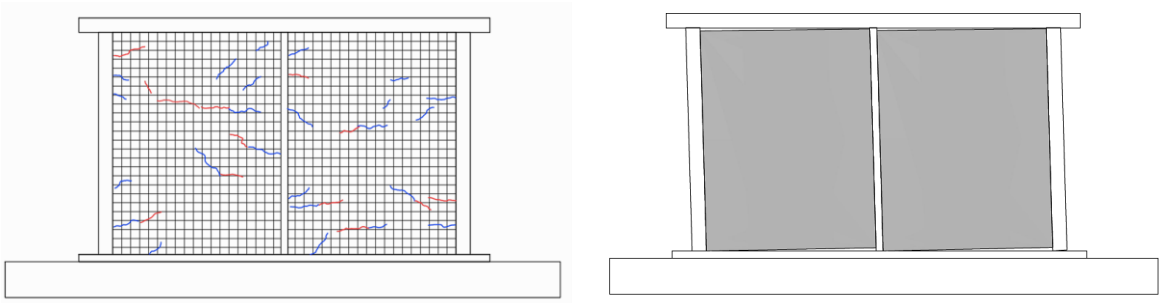

**Figure 15. (a) Crack patterns. (b) wall behaviour during the test**

The presence of nail anchors significantly influences the behavior of the brick walls connected to the timber frames. These anchors initially acted as a shear connector at the beginning of the loading cycle. However, as lateral movements increased and the walls lost bond with the timber frames, marked by the appearance of gaps, the nail anchor will act as a wall holder to keep the wall remain in place and prevented collapse, as shown in Figure 15-b. The nail functions as an anchor, attaching the infill wall to the column, and supports each other's composite action in terms of resistance to seismic loads [49]. In addition, spooning as deep as 1 cm on the wooden frame served as a location for mortar filling. The process enables excess mortars to develop good contact and bonding between the timber walls with infill, thereby increasing the lateral strength of the structure [50].

### 3.4. Stiffness and Stiffness Degradation

The average stiffness of both compressive and tensile loading at each cycle was used to calculate the sample stiffness at a certain transfer rate. The resulting stiffness degradation curve in Figure 16 shows a consistent decrease in stiffness as displacement from lateral loads increases. At the beginning, there was a slight decrease in stiffness degradation, however, from the sixth cycle onwards, the stiffness decreased steadily until the final cycle. This decrease was mainly caused by damage to the wooden joints at the nail connections. As the load was applied, the raised nails formed holes in the timber surface. The displacement should be as large as the raised nail distance for the next cycle to ensure the wall can withstand lateral loads. Additionally, the stiffness capacity is significantly influenced by the timber joints, and the presence of the infill wall [11, 51, 52].

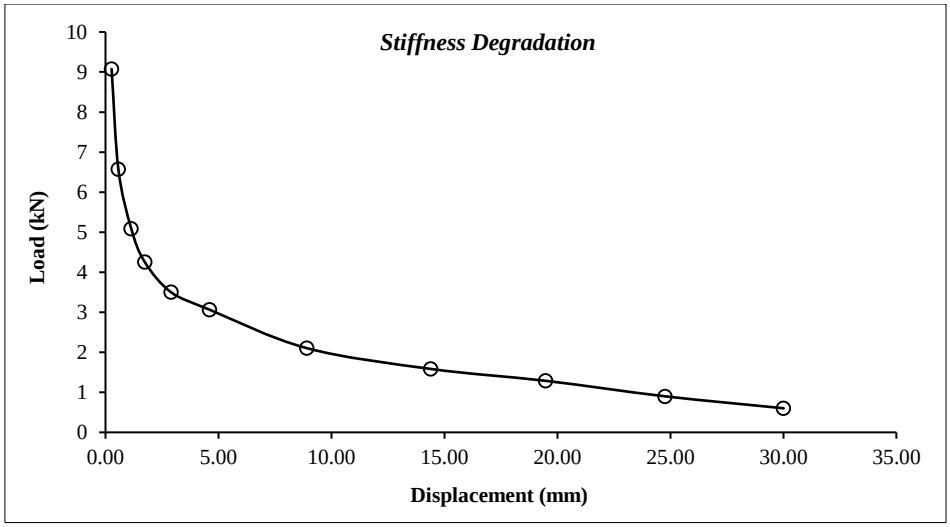


**Figure 16. Stiffness degradation of the wall**

## 3.5. Energy Dissipation

The energy dissipation of the wall was calculated at each load cycle by counting the loop in the load-transfer diagram, which is inversely related to the stiffness of the specimen. Figure 17-a, showed that at the beginning of the cycle the dissipating energy did not show a significant increase, the dissipating energy significantly increased in the sixth cycle where the bond between the timber frame and the infill wall has decreased, then the stiffness decreases significantly and the energy dissipation increases.

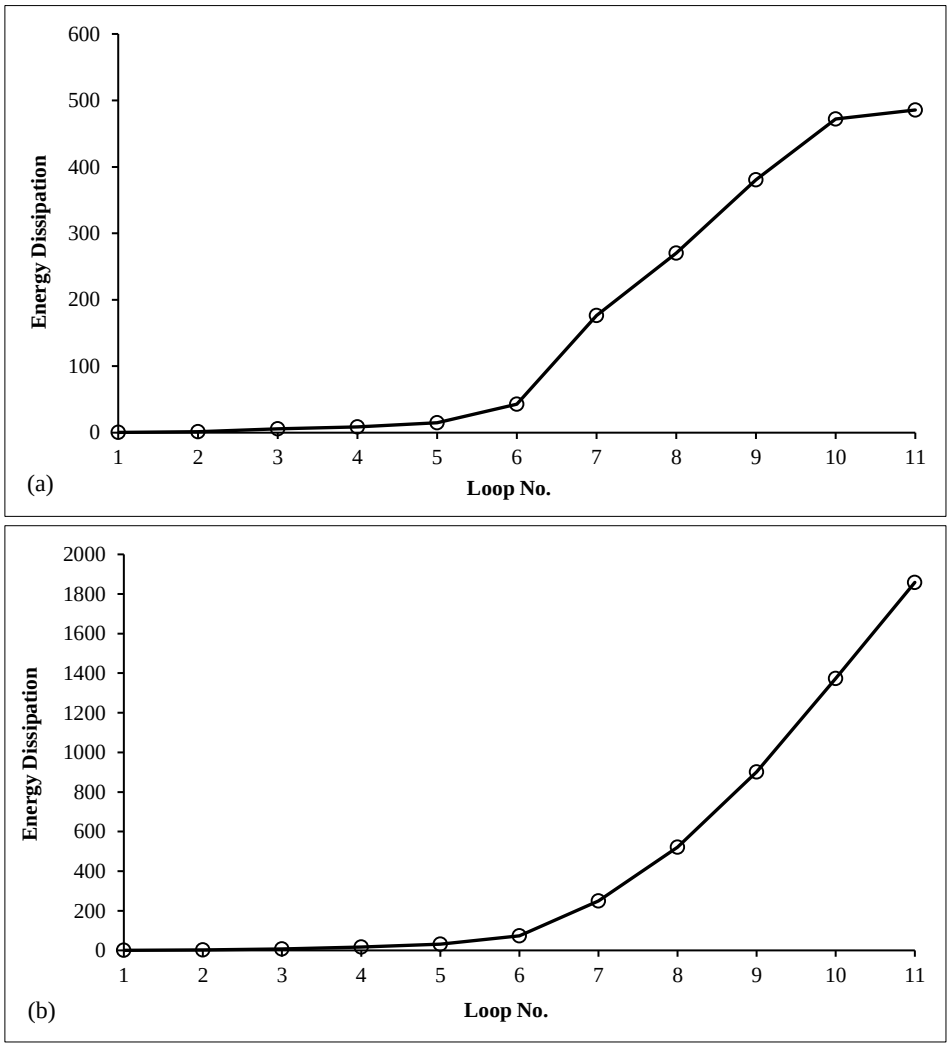


**Figure 17. (a) Energy dissipation and (b) Cumulative energy dissipation**

The energy dissipation value was relatively small at the start of the drift ratio, and continued until the 40% to 100% drift ratio. However, there was an insignificant increase for the 120% drift during the eleventh cycle. As shown in Figure 17b, the wood connection had a significant impact on the increase in energy dissipation of the test specimens. Based on diagram, the greater the loading cycle, the higher the displacement and dissipation energy influenced by wood joint, including the presence of crack on the infill wall which is beneficial for the overall building performance. The amount of energy lost during cyclic loading was attributed to the failure of the joint connection by nails [44, 46, 53], as well as the presence of the infill wall [36, 54].

## 4. Conclusion

In conclusion, the cyclic loading tests conducted on the *Kancingan* wall showed that the maximum load capacity of the test object was 26.43 kN and 28.78 kN with displacements of 19.08 mm and 15.6 mm under compressive and tensile loading, respectively. The initial stiffness was found to be 5.03 kN/mm and 9.59 kN/mm under compressive and tensile loading. The ultimate load capacity of the test object was determined to be 21.14 kN and 23.02 kN with an ultimate displacement of 30.68 mm and 25.23 mm under compressive and tensile loading, respectively. The ductility was found to be 10.76 mm and 9.78 mm under compressive and tensile loading.

The various issues found during the testing of the test object included the failure of the nail connecting tool at the column connection, the appearance of a hysteretic curve that narrowed at the waist and resulted in the lifting of the column in the seventh cycle until the end. At the 11th cycle, the wall column experienced rocking and structural failure, leading to the termination of the test. The crack patterns on the wall started to appear in the fourth cycle at a 6,46% drift and continued to worsen until the eleventh cycle, when the drift reached 104% at a displacement of 27,08 mm without the collapse of the infill walls.

The 11th loading cycle conducted during the test, with a ductility ratio >10, showed that the construction could withstand earthquake loads. However, further improvements to the wall structure of *Kancingan* house were necessary to enhance the performance. This was particularly critical for timber frame joints, which tended to experience greater damage during loading compared to brick walls due to the failure of nail connections. Except as a connector on joints, nails, serving as anchors, played a critical role in preventing the collapse of the infill walls and were carefully considered during the construction process. Additionally, even when there was a crack, the infill wall did not suffer any damage, indicating that it did not function as a load distributor but as a stiffener of the structure. For further investigation, testing the performance of *Kancingan* house walls with a wide variety of frames was recommended to obtain the best seismic performance area.

## 5. Declarations

### 5.1. Author Contributions

Conceptualization, S.O. and H.M.; methodology, N. and M.M.S.; validation, H.M., N., and M.M.S.; formal analysis, S.O.; investigation, S.O.; resources, S.O.; data curation, S.O.; writing—original draft preparation, S.O.; writing—review and editing, S.O., H.M., N., and M.M.S. All authors have read and agreed to the published version of the manuscript.

### 5.2. Data Availability Statement

The data presented in this study are available on request from the corresponding author.

### 5.3. Funding

The funding provider in this research is Lembaga Pengelola Dana Pendidikan (LPDP), Minister of Finance of Republic Indonesia.

### 5.4. Acknowledgements

Greatest gratitude to the Lembaga Pengelola Dana Pendidikan (LPDP) as the funder of this research and the Structure and Materials Laboratory at Hasanuddin University for helping provide facilities during the research.

### 5.5. Conflicts of Interest

The authors declare no conflict of interest.

## 6. References

[1] Khadka, S. S., Acharya, S., Acharya, A., & Veletzos, M. J. (2023). Enhancement of Himalayan irregular stone masonry buildings for resilient seismic design. Frontiers in Built Environment, 9. doi:10.3389/fbuil.2023.1086008.

[2] Acharya, O., Dahal, A., & Shrestha, K. C. (2023). Confined masonry in seismic regions: Application to a prototype building in Nepal. Structures, 47, 2281–2299. doi:10.1016/j.istruc.2022.12.045.

[3] Cheng, X., Zou, Z., Zhu, Z., Zhai, S., Yuan, S., Mo, Y., Chen, W., & He, J. (2020). A new construction technology suitable for frame partitioned infill walls with sliding nodes and large openings: Test results. Construction and Building Materials, 258(8), 119644. doi:10.1016/j.conbuildmat.2020.119644.

[4] Dutu, A., Gomes Ferreira, J., Guerreiro, L., Branco, F., & Gonçalves, A. M. (2012). Timbered masonry for earthquake resistance in Europe. Materiales de Construcción, 62(308), 615–628. doi:10.3989/mc.2012.01811.

[5] Goncalves, A. M., Ferreira, J. G., Guerreiro, L., & Branco, F. (2015). Experimental characterization of timber framed masonry walls cyclic behaviour. Structural Engineering and Mechanics, 53(2), 189–204. doi:10.12989/sem.2015.53.2.189.

[6] Octavia, S., Madeali, H., Junus, N., & Sir, M. M. (2024). Architectural Analysis of Rumah Kancingan in Merauke. International Journal of Technology, 15(2), 289–298. doi:10.14716/ijtech.v15i2.6687.

[7] Ren, C., Bian, R., & Li, S. (2018). On Technology and Ritual of Chuandou House Construction in Southwest China: The Case of Dong Minority Area. Built Heritage, 2(1), 39–48. doi:10.1186/BF03545701.

[8] Qu, Z., Fu, X., Kishiki, S., & Cui, Y. (2020). Behavior of masonry infilled Chuandou timber frames subjected to in-plane cyclic loading. Engineering Structures, 211, 110449. doi:10.1016/j.engstruct.2020.110449.

[9] Ergun, S. F. Y., & Schuller, M. (2021). Timber frame system after the western influence on the houses of Istanbul. Eighth Annual CHS Conference, 17-18 April, 2021, Cambridge, United Kingdom.

[10] Aktaş, Y. D., Akyüz, U., Türer, A., Erdil, B., & Güçhan, N. Ş. (2014). Seismic resistance evaluation of traditional ottoman TimberFrame Himiş houses: Frame loadings and material tests. Earthquake Spectra, 30(4), 1711–1732. doi:10.1193/011412EQS011M.

[11] Ortega, J., Vasconcelos, G., & Correia, M. (2014). An overview of the seismic strengthening techniques traditionally applied in vernacular architecture. 9th International Masonry Conference, 7-9 July, 2014, Guimarães, Portugal.

[12] Topan, A., Octavia, S., & Soleman, H. (2018). Analysis of the semi-permanent house in Merauke city in terms of aesthetic value in architecture. Journal of Physics: Conference Series, 1025, 012021. doi:10.1088/1742-6596/1025/1/012021.

[13] Octavia, S., Raubaba, H. S., Hematang, Y. I. P., & Topan, A. (2018). The Feasibility of the Kancingan House Structure in Merauke City. Proceedings of the International Conference on Science and Technology (ICST 2018), 421-425. doi:10.2991/icst-18.2018.88.

[14] Topan, A., Syanjayanta, B., Mita, M. S. W., & Makruf, A. M. A. (2023). Development of Structural Materials and House Construction in Merauke. Technium: Romanian Journal of Applied Sciences and Technology, 16, 470–474. doi:10.47577/technium.v16i.10032.

[15] Subagyono, R. R. D. J. N., Qi, Y., Chaffee, A. L., Amirta, R., & Marshall, M. (2021). Pyrolysis-gc/ms analysis of fast growing wood macaranga species. Indonesian Journal of Science and Technology, 6(1), 141–158. doi:10.17509/ijost.v6i1.31917.

[16] Heidari, A., Khaki, E., Younesi, H., & Lu, H. R. (2019). Evaluation of fast and slow pyrolysis methods for bio-oil and activated carbon production from eucalyptus wastes using a life cycle assessment approach. Journal of Cleaner Production, 241, 118394. doi:10.1016/j.jclepro.2019.118394.

[17] Tjondro, J. A. (2014). Development and prospects of wood structural engineering in Indonesia. Seminar dan Lokakarya Rekayasa Struktur, Universitas Petra, Surabaya, Indonesia. (In Indonesian).

[18] Syiemiong, H., & Marthong, C. (2021). A review on improved construction methods for clay-brick and concrete-block ordinary masonry buildings. Journal of Structural Integrity and Maintenance, 6(2), 67–83. doi:10.1080/24705314.2020.1862963.

[19] Boudaud, C., Humbert, J., Baroth, J., Hameury, S., & Daudeville, L. (2015). Joints and wood shear walls modelling II: Experimental tests and FE models under seismic loading. Engineering Structures, 101, 743–749. doi:10.1016/j.engstruct.2014.10.053.

[20] Meghlat, E. M., Oudjene, M., Ait-Aider, H., & Batoz, J. L. (2013). A new approach to model nailed and screwed timber joints using the finite element method. Construction and Building Materials, 41, 263–269. doi:10.1016/j.conbuildmat.2012.11.068.

[21] Psycharis, I. N., Pantazopoulou, S. J., & Papadrakakis, M. (2015). Seismic assessment, behavior and retrofit of heritage buildings and monuments. Springer International Publishing, Cham, Switzerland. doi:10.1007/978-3-319-16130-3.

[22] Tu, L., Cui, Z., Xu, M., Feng, Y., & Li, T. (2021). Experimental study of traditional Chuan-dou frames infilled with wood panels under in-plane cyclic load. Journal of Building Engineering, 43, 102854. doi:10.1016/j.jobe.2021.102854.

[23] Huang, H., Wu, Y., Li, Z., Sun, Z., & Chen, Z. (2018). Seismic behavior of Chuan-Dou type timber frames. Engineering Structures, 167, 725–739. doi:10.1016/j.engstruct.2017.10.072.

[24] Bağbancı, M. B., & Bağbancı, Ö. K. (2018). The Dynamic Properties of Historic Timber-Framed Masonry Structures in Bursa, Turkey. Shock and Vibration, 2018(1). doi:10.1155/2018/3257434.

[25] Hejazi, M., Hoseyni, M., & Çiftçi, A. (2022). In–plane cyclic behaviour of half-timbered walls with fired brick infill. Journal of Building Engineering, 54, 104580. doi:10.1016/j.jobe.2022.104580.

[26] Shen, Y., Yan, X., Yu, P., Liu, H., Wu, G., & He, W. (2021). Seismic resistance of timber frames with mud and stone infill walls in a Chinese traditional village dwelling. Buildings, 11(12). doi:10.3390/buildings11120580.

[27] Makarios, T., & Demosthenous, M. (2006). Seismic response of traditional buildings of Lefkas Island, Greece. Engineering Structures, 28(2), 264–278. doi:10.1016/j.engstruct.2005.08.002.

[28] Poletti, E., & Vasconcelos, G. (2015). Seismic behaviour of traditional timber frame walls: experimental results on unreinforced walls. Bulletin of Earthquake Engineering, 13(3), 885–916. doi:10.1007/s10518-014-9650-9.

[29] Ruggieri, N., & Zinno, R. (2014). Seismic assessment of "Baraccato" system: Constructive analysis and experimental investigations. Second European conference on earthquake engineering and seismology, 25-29 August, 2014, Istanbul. Turkey.

[30] Xu, R., Qi, Y., Huang, H. (2024). Experimental Study on the Seismic Performance of Traditional Timber Frame with Wattle and Daub Infill. Proceedings of the 6th International Conference on Smart Monitoring, Assessment and Rehabilitation of Civil Structures, Lecture Notes in Civil Engineering, Springer, Singapore. doi:10.1007/978-981-99-3362-4_66.

[31] Zhang, H., Tang, Z., Duan, Y., & Chen, Z. (2023). Seismic Performance of SFRC Shear Walls with Window Opening and the Substitution Effect for Steel Bars. Buildings, 13(6), 1550. doi:10.3390/buildings13061550.

[32] Octavia, S., Raubaba, H. S., & Simorangkir, Y. V. (2019). Wood and steel as a material alternative of concrete replacement in house structures in merauke city. IOP Conference Series: Earth and Environmental Science, 343(1), 012231. doi:10.1088/1755-1315/343/1/012231.

[33] Yin, J., Tang, D., Chen, T., Yang, Y., Ju, L., Wan, Y., ... & Yue, X. (2023). Seismic Risk Assessment and Rehabilitation Method of Existing RCC Structures Using Micro Concrete. Civil Engineering Journal, 9(12), 3008-3018. doi:10.28991/CEJ-2023-09-12-04.

[34] Kouris, L. A. S., & Kappos, A. J. (2012). Detailed and simplified non-linear models for timber-framed masonry structures. Journal of Cultural Heritage, 13(1), 47–58. doi:10.1016/j.culher.2011.05.009.

[35] Szczepański, M., & Migda, W. (2020). Analysis of validation and simplification of timber-frame structure design stage with PU-foam insulation. Sustainability (Switzerland), 12(15), 5990. doi:10.3390/su12155990.

[36] Xie, Q., Tong, Y., Zhang, L., Li, S., & Wang, L. (2021). Seismic Behavior of Chinese Traditional Timber Frames with Masonry Infill Wall: Experimental Tests and Hysteretic Model. International Journal of Architectural Heritage, 15(8), 1130–1144. doi:10.1080/15583058.2019.1665140.

[37] Kuantitatif, P. P. (2016). Qualitative Quantitative Research Methods and R&D. Alfabeta, Bandung, Indonesia. (In Indonesian).

[38] Susila, I. G. A. (2014). Experimental and numerical studies of masonry wall panels and timber frames of low-rise structures under seismic loadings in Indonesia. Ph.D. Thesis, The University of Manchester, Manchester, United Kingdom.

[39] ASTM E2126. (2019). Standard Test Methods for Cyclic (Reversed) Load Test for Shear Resistance of Vertical Elements of the Lateral Force Resisting Systems for Buildings. ASTM International, Pennsylvania, United States. doi:10.1520/E2126-19.

[40] Shen, Y., Yan, X., Liu, H., Wu, G., & He, W. (2022). Enhancing the In-Plane Behavior of a Hybrid Timber Frame–Mud and Stone Infill Wall Using PP Band Mesh on One Side. Polymers, 14(4), 773. doi:10.3390/polym14040773.

[41] Ruggieri, N., Tampone, G., & Zinno, R. (2015). In-Plane Versus Out-of-Plane "behavior" of an Italian Timber Framed System - The Borbone Constructive System: Historical Analysis and Experimental Evaluation. International Journal of Architectural Heritage, 9(6), 696–711. doi:10.1080/15583058.2015.1041189.

[42] Xue, S., Liu, X., Wang, Y., & Zhou, H. (2021). Lateral force resistance of structural insulated panels consisting of wood-based sheathing and a polyurethane core. Journal of Building Engineering, 40. doi:10.1016/j.jobe.2021.102317.

[43] Gonçalves, A. M., Ferreira, J. G., Guerreiro, L., & Branco, F. (2013). numerical modelling and experimental characterization of pombalino "frontal" wall cyclic behavior. 4th International Conference on Integrity, Reliability and Failure, 23-27 June, Funchal, Portugal.

[44] Kildashti, K., Alinoori, F., Moshiri, F., & Samali, B. (2021). Computational simulation of light timber framing connections strengthened with self-tapping screws. Journal of Building Engineering, 44(March), 103003. doi:10.1016/j.jobe.2021.103003.

[45] Dutu, A., Sakata, H., & Yamazaki, Y. (2017). Comparison between different types of connections and their influence on timber frames with masonry infill structures' seismic behavior. 16th Conference on Earthquake Engineering, 9-13 January, 2017, Santiago, Chile.

[46] Vasconcelos, G., Poletti, E., Salavessa, E., Jesus, A. M. P., Lourenço, P. B., & Pilaon, P. (2013). In-plane shear behaviour of traditional timber walls. Engineering Structures, 56, 1028–1048. doi:10.1016/j.engstruct.2013.05.017.

[47] Vieux-Champagne, F., Sieffert, Y., Grange, S., Polastri, A., Ceccotti, A., & Daudeville, L. (2014). Experimental analysis of seismic resistance of timber-framed structures with stones and earth infill. Engineering Structures, 69, 102–115. doi:10.1016/j.engstruct.2014.02.020.

[48] Langenbach, R. (2007). From "Opus Craticium" to the "Chicago frame": Earthquake-resistant traditional construction. International Journal of Architectural Heritage, 1(1), 29–59. doi:10.1080/15583050601125998.

[49] Hutajulu, M., Tarigan, J., & Tarigan, P. (2019). Analisa Pushover dan Eksperimen Struktur Portal dengan Dinding Batubata dengan Menggunakan Angkur pada Kolom dan Balok pada Non Engineered Building. Media Komunikasi Teknik Sipil, 24(2), 158. doi:10.14710/mkts.v24i2.19914.

[50] Wadi, H., Amziane, S., Toussaint, E., & Taazount, M. (2019). Lateral load-carrying capacity of hemp concrete as a natural infill material in timber frame walls. Engineering Structures, 180, 264–273. doi:10.1016/j.engstruct.2018.11.046.

[51] Dutu, A., Sakata, H., Yamazaki, Y., & Shindo, T. (2016). In-Plane Behavior of Timber Frames with Masonry Infills under Static Cyclic Loading. Journal of Structural Engineering, 142(2), 1–18. doi:10.1061/(asce)st.1943-541x.0001405.

[52] Benavent-Climent, A., Ramírez-Márquez, A., & Pujol, S. (2018). Seismic strengthening of low-rise reinforced concrete frame structures with masonry infill walls: Shaking-table test. Engineering Structures, 165, 142–151. doi:10.1016/j.engstruct.2018.03.026.

[53] Casagrande, D., Polastri, A., Sartori, T., Loss, C., & Chiodega, M. (2016). Experimental campaign for the mechanical characterization of connection systems in the seismic design of timber buildings. World Conference on Timber Engineering (WCTE), 22-25 August, 2016, Vienna, Austria.

[54] Parisse, F., Poletti, E., Dutu, A., & Rodrigues, H. (2021). Numerical modeling of the seismic performance of Romanian timber-framed masonry walls. Engineering Structures, 239. doi:10.1016/j.engstruct.2021.112272.